Synthesis and Characterisation of Guaiazulene Derivatives of Two Ruthenium Carbonyl Clusters†

Brian F. G. Johnson,[*,a] **Douglas S. Shephard,**[a] **Andrew J. Edwards,**[c] **Dario Braga,**[*,b] **Emilio Parisini**[b] **and Paul R. Raithby**[c]
[a] *Department of Chemistry, The University of Edinburgh, West Mains Road, Edinburgh EH9 3JJ, UK*
[b] *Dipartimento di Chimica 'G. Ciamician', dell'Università di Bologna, Via Selmi 2, 40126 Bologna, Italy*
[c] *Department of Chemistry, The University of Cambridge, Lensfield Road, Cambridge CB2 1EW, UK*

Thermolysis of $[Ru_3(CO)_{12}]$ **1** in octane with guaiazulene (7-isopropyl-1,4-dimethylazulene) gave $[Ru_3(CO)_7(\mu_3\text{-}\eta^5{:}\eta^3{:}\eta^3\text{-}C_{15}H_{18})]$ **2** and $[Ru_4(CO)_9(\mu_3\text{-}\eta^5{:}\eta^3{:}\eta^3\text{-}C_{15}H_{18})]$ **3**. The products **2** and **3** have been characterised by spectroscopic techniques and by single-crystal X-ray diffraction. Comparison is made between the two structures of the cluster compounds. Proton NMR and crystal structural data indicate an increased degree of metal–hydrocarbon interaction in **3**.

Reports of carbonyl cluster compounds containing azulene or its derivatives are few,[1] and to our knowledge cluster-co-ordinated guaiazulene (7-isopropyl-1,4-dimethylazulene) is unknown. This study represents a continuation of our study into cluster-co-ordinated carbocycles. The fused five- and seven-membered rings which constitute the azulene moiety provide us with the possibility of direct comparison of the two bonding modes between five- and seven-co-ordination. Variance of cluster nuclearity has been shown to be a reliable probe into electronic effects governing arene–cluster bonding.[2] The co-ordination of derivatised carbocycles of this type also provides the possibility of asymmetric synthesis, the study of which is currently underway. The aim of this paper is two-fold: to consolidate the chemistry of cluster-bound fused carbocycles and to extend this field by way of introducing asymmetry.

Results and Discussion

Thermolysis of $[Ru_3(CO)_{12}]$ **1** in octane with guaiazulene $(C_{15}H_{18})$ gives the two new clusters $[Ru_3(CO)_7(\mu_3\text{-}\eta^5{:}\eta^3{:}\eta^3\text{-}C_{15}H_{18})]$ **2** and $[Ru_4(CO)_9(\mu_3\text{-}\eta^5{:}\eta^3{:}\eta^3\text{-}C_{15}H_{18})]$ **3** in moderate yield. The two compounds are air-stable both in solution and in the solid state. In each case, separation was achieved by thin-layer chromatography using dichloromethane–hexane (3:7 v/v) as eluent and preliminary characterisation was by means of their solution infrared spectra in dichloromethane and positive-ion fast atom bombardment mass spectra. Both compounds showed absorptions in the terminal and bridging carbonyl regions in solution immediately after separation. However, no μ-CO was detected in the solid-state infrared spectrum of **3** or in a solution infrared spectrum from crystals of **3**, consistent with its structure as determined in the solid state (see below). This strongly suggests, therefore, that the initial solution and solid-state carbonyl distributions in **3** are not the same. An apparent driving force for this stereochemical rearrangement is the unequal electron donation from the guaiazulene ligand to the cluster face [Ru(1), Ru(2), Ru(3)]. The energy required for such a structural transformation can be assumed to be relatively low. The mass spectrum of each compound showed the molecular ion and a carbonyl regression appropriate to the number of carbonyls carried by the cluster.

Table 1 Proton NMR data for compounds **2** and **3**

	δ				
^1H Nucleus	**2**	**3**	Multiplicity	Integral	J/Hz
H(2) C_5 ring	5.73	5.94	d	1	3
H(3) C_5 ring	4.59	4.19	d	1	3
H(6) C_7 ring	4.79	3.99	s	1	—
H(8) C_7 ring	2.20	1.67	d	1	7
H(9) C_7 ring	5.35	5.07	d	1	7
H(11) Me	1.87	1.74	s	3	—
H(12) Pr^i	2.34	2.48	d of q	1	7
H(13, 14) Pr^i	1.46, 1.21	1.51, 1.23	d	3, 3	7
H(15) Me	1.98	1.17	s	3	—

The solution ^1H NMR spectra of compounds **2** and **3** show the same number and type of resonances and similar coupling constants. However, the protons in positions proximal to the cluster-bound carbon framework show significant differences in chemical shift, presumably symptomatic of the two different cluster nuclearities involved. Assignment of the spectral features for **2** and **3** was aided by various decoupling and nuclear Overhauser effect (NOE) experiments. The chemical shifts of corresponding protons in both compounds are given in Table 1. Comparison of these two sets of data shows predominantly lower values for **3** with two exceptions: H(2) and the signals due to the isopropyl group which are very similar. A reduction in the ring current and concomitant lowering of chemical shift has been previously observed for transition-metal-bonded arenes.[3] It has also been noted that facially bonded arenes have lower chemical shifts than those that are apically bound.[3] This has been ascribed to a different hybridisation at the metal-bound carbons, from sp^2 to sp^3, and the consequential increase in diamagnetic shielding. The lowest chemical shift for a ring proton in each case is H(8) (see Table 1). It is bound to carbon C(8) in the C_7 ring, as seen in the solid-state structures (see below), which in turn is bonded to two metal atoms [Ru(2), Ru(3)] and deviates greatly from the C_7 plane. Rotation of the isopropyl groups in solution is severely hindered, since the two methyl groups C(13) and C(14) give rise to individual signals and a corresponding doublet of quartets was observed for H(12).

Solid-state Structures of Compounds **2** *and* **3**.—Representations of the solid-state molecular structures of compounds **2**

---

† *Supplementary data available:* see Instructions for Authors, *J. Chem. Soc., Dalton Trans.*, 1995, Issue 1, pp. xxv–xxx.

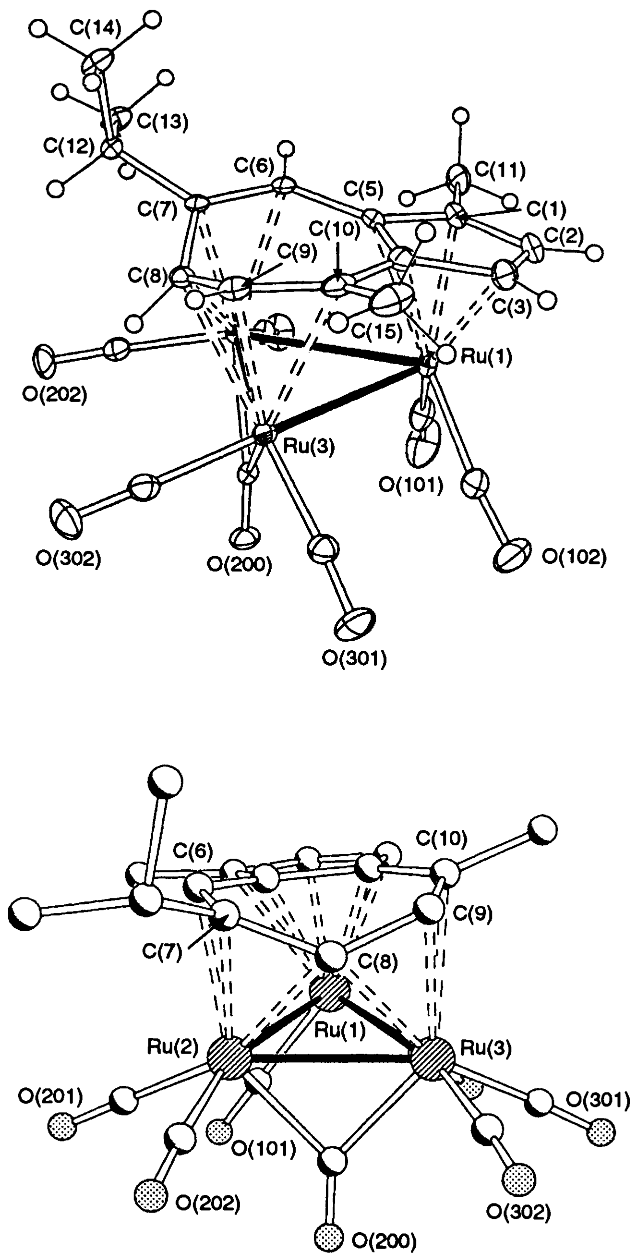

Fig. 1 Two views of the solid-state molecular structure of compound 2

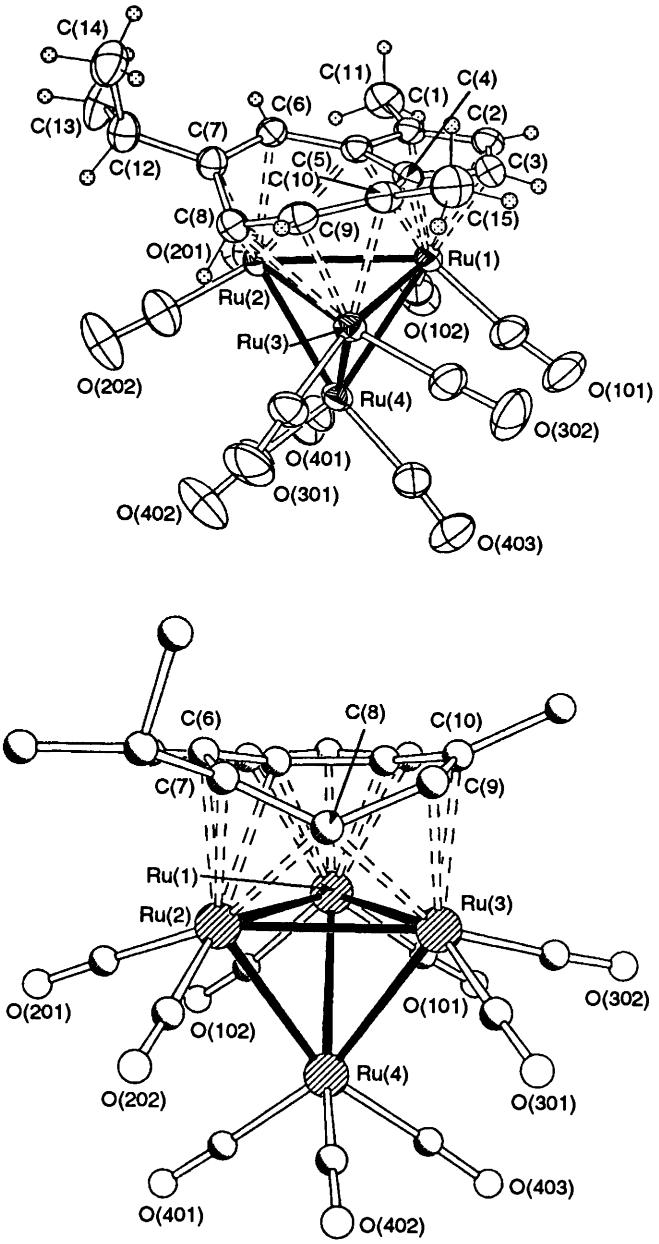

Fig. 2 Two views of the solid-state molecular structure of compound 3

and 3 are given in Figs. 1 and 2 respectively and selected bond lengths and angles are given in Tables 2 and 3. Both crystal structures belong to centrosymmetric space groups, hence both enantiomers exist for each compound. Each carbon in the fused rings of **2** and **3** is chemically and crystallographically unique and chiral. The azulene framework donates a total of ten electrons to the Ru_3 and Ru_4 clusters producing standard electron counts of 48 and 60 respectively.

The co-ordination mode shown by the bicyclic ligand over a trimetal face is in accordance with that previously observed.[1] The carbon–carbon distances for compounds **2** and **3** are shown in Fig. 3. Close inspection of the C_5 ring bond lengths reveals significant deviation from a regular pentagon in each case. This distortion is greatest in **3**: possibly a consequence of higher nuclearity. The bridgehead bond length is appreciably longer in **2** and **3** than that found in other cyclopentadienyl derivatives. The modification is such that the largest internal angles are at C(1), C(2) and C(3) for both compounds. The averaged plane defined by the C_5 ring is not parallel with that of the ruthenium triangle but is tilted such that the two planes produce an angle of 12.2 and 2.0° for **2** and **3** respectively. The longest Ru(1) to C_5 ring distance is 2.267(4) Å [Ru(1)–C(1)] in **2** and 2.308(5) Å [Ru(1)–C(5)] in **3**, while the shortest is 2.211(4) Å [Ru(1)–C(4)] in **2** and 2.208(6) Å [Ru(1)–C(3)] in **3**.

The variation in the C–C bond lengths of the C_7 rings is more pronounced. Delocalisation around the C_7 ring is unlikely in view of this variation and the unfavourable stereochemistry. The shortest C–C bonds in both compounds, C(6)–C(7) and C(9)–C(10), compare favourably with those found in co-ordinated olefins and suggest localisation of electron density at these sites. The remaining bonds are significantly longer.

The deviation from planarity in the C_7 ring is greater than that in the C_5 ring. An 'envelope flap' type distortion, with C(8) at the apex, produces fold angles of 138.4 and 133.7° for compounds **2** and **3** respectively. The Ru(2)–C(8) distance is significantly shorter than the Ru(3)–C(8) distance in each compound. A formal description of the carbon–metal bonding for C(8) is not straightforward and comparable examples are few; however, a similar bonding mode has been elucidated in a dinickel compound.[4] The said interaction may be classified as a

Table 2 Selected bond lengths (Å) and angles (°) for compound **2**

Ru(1)–Ru(3)	2.9009(8)	Ru(1)–C(101)	1.882(5)
Ru(1)–Ru(2)	2.9362(6)	Ru(2)–C(202)	1.857(4)
Ru(2)–Ru(3)	2.7383(9)	Ru(2)–C(201)	1.889(4)
Ru(1)–C(4)	2.211(4)	Ru(2)–C(200)	2.084(4)
Ru(1)–C(3)	2.230(4)	Ru(3)–C(302)	1.867(4)
Ru(1)–C(2)	2.254(4)	Ru(3)–C(301)	1.869(4)
Ru(1)–C(5)	2.249(4)	Ru(3)–C(200)	2.033(4)
Ru(1)–C(1)	2.267(4)	C(101)–O(101)	1.139(6)
Ru(2)–C(7)	2.254(3)	C(102)–O(102)	1.144(5)
Ru(2)–C(6)	2.355(4)	C(200)–O(200)	1.172(5)
Ru(2)–C(8)	2.389(4)	C(201)–O(201)	1.144(5)
Ru(3)–C(9)	2.284(4)	C(202)–O(202)	1.147(5)
Ru(3)–C(8)	2.458(4)	C(301)–O(301)	1.148(5)
Ru(3)–C(10)	2.536(4)	C(302)–O(302)	1.132(5)
Ru(1)–C(102)	1.884(4)		
Ru(3)–C(200)–Ru(2)	83.36(14)	C(6)–C(7)–C(8)	120.9(3)
Ru(3)–Ru(1)–Ru(2)	55.95(2)	C(6)–C(7)–C(12)	122.3(3)
Ru(2)–Ru(3)–Ru(1)	62.68(2)	C(8)–C(7)–C(12)	116.7(3)
Ru(3)–Ru(2)–Ru(1)	61.37(2)	C(9)–C(8)–C(7)	126.9(3)
C(2)–C(1)–C(5)	108.5(4)	C(10)–C(9)–C(8)	126.3(4)
C(2)–C(1)–C(11)	126.0(4)	C(9)–C(10)–C(4)	122.4(4)
C(5)–C(1)–C(11)	125.4(4)	C(9)–C(10)–C(15)	119.9(4)
C(3)–C(2)–C(1)	109.1(4)	C(4)–C(10)–C(15)	117.3(4)
C(2)–C(3)–C(4)	108.9(4)	O(101)–C(101)–Ru(1)	176.2(4)
C(3)–C(4)–C(10)	123.7(4)	O(102)–C(102)–Ru(1)	173.4(4)
C(3)–C(4)–C(5)	106.7(4)	O(200)–C(200)–Ru(3)	140.5(3)
C(10)–C(4)–C(5)	129.5(3)	O(200)–C(200)–Ru(2)	136.1(3)
C(6)–C(5)–C(1)	123.1(3)	O(201)–C(201)–Ru(2)	178.5(3)
C(6)–C(5)–C(4)	129.9(4)	O(202)–C(202)–Ru(2)	177.0(3)
C(1)–C(5)–C(4)	106.8(3)	O(301)–C(301)–Ru(3)	175.6(4)
C(7)–C(6)–C(5)	125.5(3)	O(302)–C(302)–Ru(3)	176.3(4)

Table 3 Selected bond lengths (Å) and angles (°) for compound **3**

Ru(1)–Ru(3)	2.8649(8)	R(1)–C(102)	1.864(7)
Ru(2)–Ru(4)	2.7111(10)	Ru(1)–C(101)	1.869(8)
Ru(2)–Ru(3)	2.8734(8)	Ru(2)–C(202)	1.853(8)
Ru(2)–Ru(1)	2.9128(8)	Ru(2)–C(201)	1.869(7)
Ru(4)–Ru(3)	2.6875(13)	Ru(3)–C(301)	1.835(7)
Ru(4)–Ru(1)	2.8413(8)	Ru(3)–C(302)	1.849(7)
Ru(1)–C(3)	2.208(6)	Ru(4)–C(402)	1.837(8)
Ru(1)–C(2)	2.239(6)	Ru(4)–C(403)	1.903(8)
Ru(1)–C(1)	2.260(5)	Ru(4)–C(401)	1.922(8)
Ru(1)–C(4)	2.289(6)	C(202)–O(202)	1.121(11)
Ru(1)–C(5)	2.308(5)	C(201)–O(201)	1.131(9)
Ru(3)–C(9)	2.202(6)	C(401)–O(401)	1.111(11)
Ru(3)–C(10)	2.275(6)	C(402)–O(402)	1.139(10)
Ru(3)–C(8)	2.451(6)	C(403)–O(403)	1.138(10)
Ru(2)–C(7)	2.207(6)	C(101)–O(101)	1.137(10)
Ru(2)–C(6)	2.248(6)	C(102)–O(102)	1.156(10)
Ru(2)–C(8)	2.388(6)	C(301)–O(301)	1.153(8)
Ru(2)–C(5)	2.598(6)	C(302)–O(302)	1.146(9)
Ru(2)–Ru(4)–Ru(1)	63.23(2)	C(6)–C(7)–C(8)	120.0(5)
Ru(4)–Ru(1)–Ru(3)	56.19(3)	C(6)–C(7)–C(12)	122.1(5)
Ru(4)–Ru(1)–Ru(2)	56.20(2)	C(8)–C(7)–C(12)	117.7(5)
Ru(3)–Ru(1)–Ru(2)	59.64(2)	C(9)–C(8)–C(7)	125.9(5)
Ru(4)–Ru(2)–Ru(3)	57.45(3)	C(10)–C(9)–C(8)	124.2(5)
Ru(4)–Ru(2)–Ru(1)	60.57(2)	C(9)–C(10)–C(4)	121.6(5)
Ru(3)–Ru(2)–Ru(1)	59.35(2)	C(9)–C(10)–C(15)	119.1(6)
Ru(3)–Ru(4)–Ru(2)	64.31(3)	C(4)–C(10)–C(15)	118.8(6)
Ru(3)–Ru(4)–Ru(1)	62.35(2)	C(13)–C(12)–C(14)	110.6(7)
C(2)–C(1)–C(5)	108.7(5)	C(13)–C(12)–C(7)	114.7(6)
C(2)–C(1)–C(11)	126.5(6)	C(14)–C(12)–C(7)	108.2(6)
C(5)–C(1)–C(11)	124.6(6)	O(202)–C(202)–Ru(2)	176.7(10)
C(1)–C(2)–C(3)	108.3(5)	O(201)–C(201)–Ru(2)	177.1(7)
C(2)–C(3)–C(4)	110.2(5)	O(401)–C(401)–Ru(4)	177.3(8)
C(3)–C(4)–C(10)	124.6(5)	O(402)–C(402)–Ru(4)	176.3(9)
C(3)–C(4)–C(5)	105.7(5)	O(403)–C(403)–Ru(4)	174.4(8)
C(10)–C(4)–C(5)	129.5(5)	O(101)–C(101)–Ru(1)	172.9(8)
C(6)–C(5)–C(1)	122.9(5)	O(102)–C(102)–Ru(1)	167.3(7)
C(6)–C(5)–C(4)	129.5(5)	O(301)–C(301)–Ru(3)	179.0(6)
C(1)–C(5)–C(4)	107.0(5)	O(302)–C(302)–Ru(3)	177.4(8)
C(7)–C(6)–C(5)	124.4(5)		

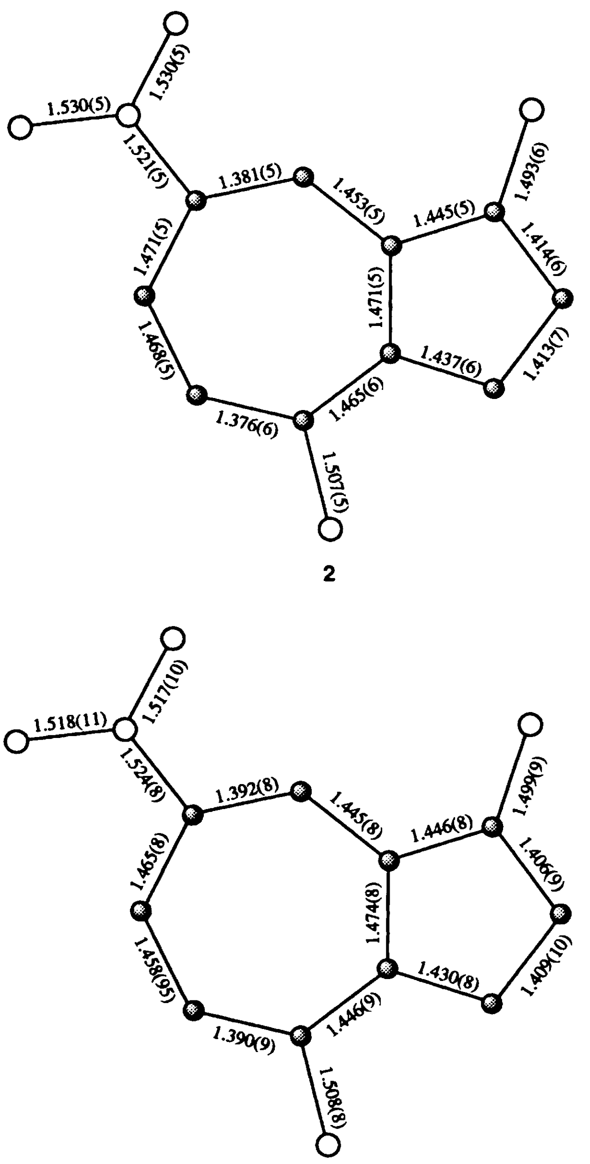

2

3

Fig. 3 Representation of the carbon framework bond lengths of compounds **2** and **3** in the solid state

'three-centre three-electron' bond. The metal–ligand distances vary greatly for the non-bridgehead carbons of the C_7 ring. For **2** they lay in the range 2.536(4) [Ru(3)–C(10)] to 2.254(3) Å [Ru(2)–C(7)]. The Ru(2)–C(6) bond is significantly shorter than the corresponding Ru(3)–C(10) distance. This is part of an asymmetric distortion where all Ru(2)–C_7 bonds are shorter than their related Ru(3)–C_7 bonds. This could be due to different electronic effects of the substituent groups [Pr^i at C(7) and Me at C(10)].

The C_7 ring–metal bonding in compound **3** gives a different picture. The six bond lengths corresponding to those in **2** lay in the range 2.451(6) [Ru(3)–C(8)] to 2.202(6) Å [Ru(3)–C(9)]. The Ru(3)–C(10) distance [2.275(6) Å] is very much shorter, showing a stronger metal–carbon interaction consistent with the lengthening of the C(10)–C(9) bond (*cf.* **2**). The C_7 ring bonds to Ru(2) also indicate an increased degree of metal–carbon interaction compared to **2**, in particular, bonds Ru(2)–C(6) and Ru(2)–C(7). Likewise, these distances correspond with a larger C(6)–C(7) distance observed in **3**. Atom Ru(2) has a possible fourth bonding interaction with C(5). At 2.598(6) Å this is rather weak; however, such an interaction would aid electron-density distribution across the cluster framework.

Metal–metal interactions in cluster compounds are often referred to as 'soft'. Hence metal–metal distances can be expected to vary such that they optimise the 'harder' metal–ligand bonding. The intermetallic distances in **2** show a distinct pattern of two long [Ru(1)–Ru(2) and Ru(1)–Ru(3)] and one short [Ru(2)–Ru(3)] spanning the C_7 ring and bridged by a single μ-CO [C(200)–O(200)]. The shortening of this bond could be to maximise orbital overlap of Ru(2) and Ru(3) with the μ-CO and the C_7 ring and compensate for the formal electron deficiency at these atoms. Atom Ru(1) is formally electron rich, thus electron density must be donated to Ru(2) and Ru(3) along the polar intermetallic bonds.

The tetrahedral cluster core of compound **3** deviates from ideality. The triruthenium face co-ordinated to the fused carbocycles is distorted in a manner different from that of **2**. The shortest bond is Ru(1)–Ru(3) and not Ru(2)–Ru(3) as in **2**. This could be due to a compensatory effect of Ru(4) subtending the metal face. The metal contacts to Ru(4) are shorter than those between the remaining metal atoms, in particular Ru(2)–Ru(4) and Ru(3)–Ru(4). Atoms Ru(2) and Ru(3) are formally more electron deficient than Ru(1), therefore it appears that these shortened contacts represent a system by which this is counterbalanced.

Together with the bridging CO, six terminal carbonyls, two on each metal, make up the ligand cage of compound **2**. The CO bond lengths lie in the range 1.148(5) [C(301)–O(301)] to 1.132(5) Å [C(302)–O(302)]. In **3** all nine CO ligands are terminal in the solid state. Atoms Ru(1), Ru(2) and Ru(3) each carry two whilst Ru(4) is bound to three. The shortest C–O bond length is found on the carbonyl attached to Ru(4), roughly *trans* to the Ru(1)–Ru(4) contact. The largest C–O distance is found in a carbonyl attached to Ru(1). This is likely to be due to a consequence of π-back bonding from the electron-rich metal.

The solid-state intermolecular interactions of compounds **2** and **3** are shown in Figs. 4 and 5 respectively. In each case they appear to be dominated by the CO · · · H type. In **2** the shortest of these interactions is between the oxygen atom of the μ-CO and H(2) (2.29 Å). Packing phenomena of this type have been shown to be instrumental in the ordering of similar cluster compounds in the solid state.[5] Two further interactions of the CO · · · H type exist in the crystal structure of **2**, namely H(15b) · · · O(201) (2.53 Å) and H(9) · · · O(102) (2.57 Å). The solid-state architecture of **3** consists of alternate layers of each enantiomer. The two interactions observed are found exclusively between molecules of common chirality. The *ipso*-hydrogen of the cyclopentadienyl moiety is again involved in a CO · · · H type interaction [H(2) · · · O(302) 2.54 Å], whilst the second CO · · · H contact is between that of a methyl hydrogen [H(11b)] and O(301) (2.58 Å). It should be noted that no graphitic-like interactions are observed in crystalline **2** or **3** as has been observed in many arene clusters.[5] This is perhaps due to the inauspicious steric requirements of the substituent groups.

Conclusion

The azulene derivative guaiazulene is able to co-ordinate in a facial mode on both Ru_3 and Ru_4 clusters. Asymmetry of the hydrocarbon induces variations in the nature of the metal–carbon bonds. The presence of the fourth metal atom in **3** appears to facilitate cluster–hydrocarbon interaction. As a consequence of this the ^1H NMR spectrum of **3** shows a general shift to lower frequencies and small but significant alterations to the carbon framework of the fused bicyclic ligand are observed.

Experimental

All reactions were carried out with the exclusion of air using

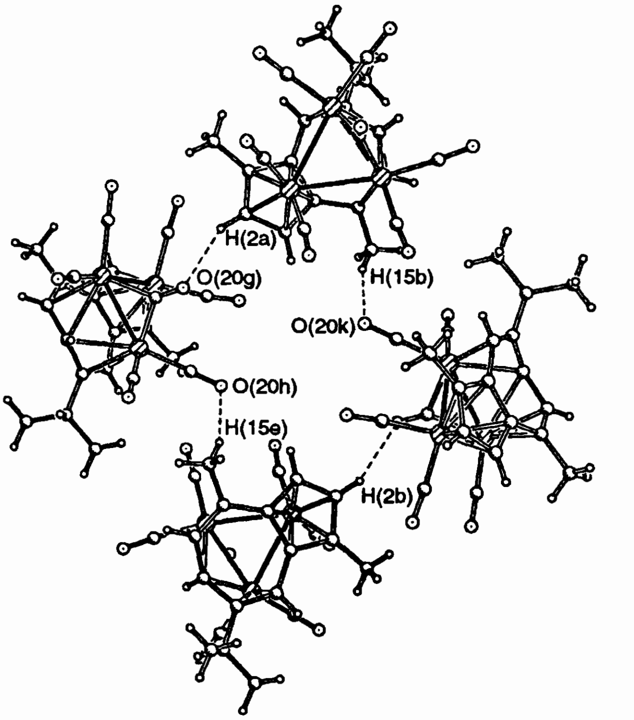

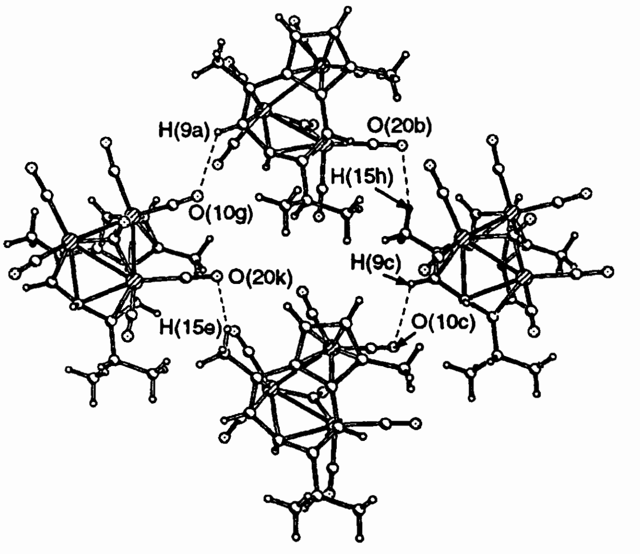

Fig. 4 Solid-state intermolecular interactions observed in compound **2**

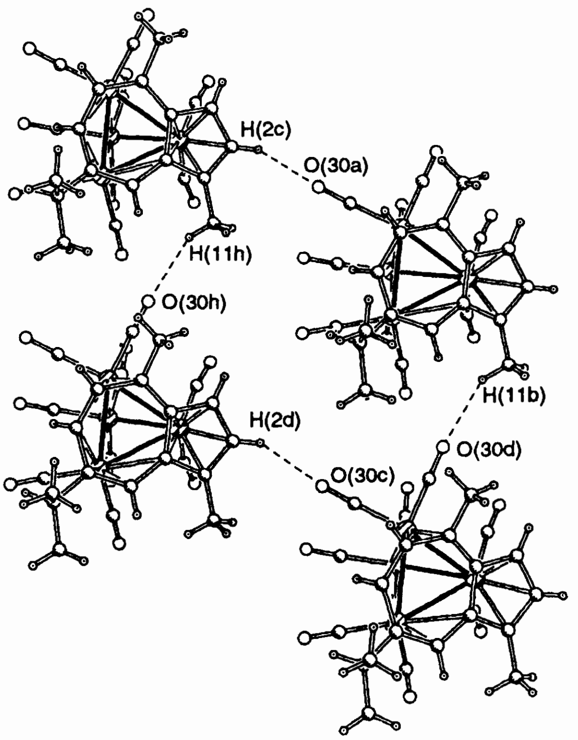

Fig. 5 'Intra-layer' solid-state intermolecular interactions observed in compound **3**

solvents distilled under a nitrogen atmosphere. Subsequent product work-up was achieved without precautions to exclude air. The IR spectra were recorded on a Perkin-Elmer 1710 series FTIR instrument in CH_2Cl_2 using NaCl cells (path length 0.5 mm), positive-ion fast atom bombardment mass spectra using a Kratos MS50TC spectrometer and CsI as calibrant and ^1H NMR spectra in $CDCl_3$ using a Bruker AM400 instrument referenced to internal $SiMe_4$. Products were separated by thin-layer chromatography (TLC) using plates supplied by Merck (0.25 mm layer of Kieselgel 60 F_{254}). The compound $[Ru_3(CO)_{12}]$ **1** was prepared using a standard procedure. Guaiazulene was obtained from Aldrich and used without further purification.

Preparation and Characterisation of $[Ru_3(CO)_7(\mu_3\text{-}\eta^5:\eta^3:\eta^3\text{-}C_{15}H_{18})]$ **2** *and* $[Ru_4(CO)_9(\mu_3\text{-}\eta^5:\eta^3:\eta^3\text{-}C_{15}H_{18})]$ **3**.—Compound **1** (1.00 g) was placed in a round-bottom flask (50 cm^3) equipped with a magnetic follower. Guaiazulene (2 cm^3) and octane (20 cm^3) were added and the mixture refluxed under dry Ar for 4.5 h. The flask was allowed to cool to ambient temperature, after which the solvent was removed *in vacuo*. The products were separated by silica-column chromatography. Elution with hexane gave a dark blue band of unreacted guaiazulene and some **1**. Further elution with dichloromethane–hexane (1 : 3) gave two orange bands, **2** (190 mg) and **3** (270 mg). Elution with dichloromethane gave small amounts of a dark and as yet uncharacterised product. Compounds **2** and **3** were initially characterised on the basis of their infrared and positive-ion fast atom bombardment spectra. Crystals of **2** suitable for X-ray structural determination were grown by layering hexane on a concentrated solution in dichloromethane and allowing slow diffusion to occur under ambient conditions in the absence of light. Single crystals of **3** were grown from a solution of dichloromethane–toluene (1 : 1) by slow diffusion of pentane onto the solution at 248 K.

Compound **2**: IR (CH_2Cl_2) ν(CO) 2078m, 2036s, 2001vs, 1962w, 1947w and 1766w (br); (KBr) 2032s, 2000 (sh), 1985vs, 1948vs, 1925s, 1904s and 1771s cm^{-1}; ^1H NMR ($CDCl_3$, 298 K) δ 5.73 (d, 1 H, $J = 3$), 5.35 (d, 1 H, $J = 8$), 4.79 ('s', 1 H), 4.59 (d, 1 H, $J = 3$), 2.34 (d of q, 1 H, $J = 7$), 2.20 ('d', 1 H, $J = 7$), 1.87 (s, 3 H), 1.49 (s, 3 H), 1.46 (d, 3 H, $J = 7$) and 1.21 (d, 3 H, $J = 7$ Hz); m/z 699 (calc. for M^+: 698) (Found: C, 38.0; H, 2.65. Calc. for $C_{22}H_{18}O_7Ru_3$: C, 37.9; H, 2.60%).

Compound **3**: IR (CH_2Cl_2) ν(CO) 2054s, 1996vs, 1956w, 1925w and 1770w (br); (KBr) 2051s, 2038s, 1989vs, 1977vs, 1952s and 1914s cm^{-1}; ^1H NMR ($CDCl_3$, 298 K) δ 5.94 (d, 1 H, $J = 3$), 5.07 (d, 1 H, $J = 8$), 4.19 (d, 1 H, $J = 3$), 3.99 ('s', 1 H), 2.48 (d of q, 1 H, $J = 7$), 1.74 (s, 3 H), 1.67 (d, 1 H, $J = 7$), 1.51 (d, 3 H, $J = 7$), 1.23 (d, 3 H, $J = 7$ Hz) and 1.17 (s, 3 H); m/z 856 (calc. for M^+: 855) (Found: C, 33.7; H, 2.10. Calc. for $C_{24}H_{18}O_9Ru_4$: C, 33.75; H, 2.10%).

Crystallography.—Crystal data for compound **2**. $C_{22}H_{18}O_7Ru_3$, $M = 697.57$, monoclinic, space group $P2_1/n$,

Table 4 Atomic coordinates (× 10^4) for compound **2**

Atom	x	y	z
Ru(1)	1524(1)	1971(1)	7243(1)
Ru(2)	−1006(1)	2704(1)	7316(1)
Ru(3)	329(1)	2962(1)	5723(1)
C(1)	812(4)	634(3)	7861(3)
C(2)	1993(4)	472(3)	7478(3)
C(3)	1946(4)	652(3)	6509(3)
C(4)	721(4)	953(3)	6259(3)
C(5)	−13(3)	930(2)	7119(3)
C(6)	−1324(3)	1098(2)	7254(3)
C(7)	−2098(3)	1557(2)	6638(2)
C(8)	−1596(3)	2068(2)	5840(3)
C(9)	−727(4)	1720(3)	5141(3)
C(10)	362(4)	1257(3)	5320(3)
C(11)	447(4)	464(3)	8848(3)
C(12)	−3500(3)	1508(3)	6707(3)
C(13)	−3992(4)	1449(3)	7702(3)
C(14)	−3955(4)	691(3)	6120(3)
C(15)	1156(4)	943(3)	4521(3)
C(101)	1647(4)	2728(3)	8307(3)
O(101)	1792(3)	3183(3)	8947(3)
C(102)	2882(4)	2666(3)	6824(3)
O(102)	3773(3)	3044(3)	6632(3)
C(200)	138(3)	3772(3)	6871(3)
O(200)	455(3)	4490(2)	7165(2)
C(201)	−956(4)	2901(3)	8620(3)
O(201)	−943(3)	3036(2)	9407(2)
C(202)	−2382(4)	3471(3)	7260(3)
O(202)	−3211(3)	3961(2)	7190(2)
C(301)	1750(4)	3465(3)	5190(3)
O(301)	2577(3)	3823(2)	4848(2)
C(302)	−568(4)	3756(3)	4945(3)
O(302)	−1151(3)	4249(2)	4514(2)

$a = 10.808(2)$, $b = 14.488(3)$, $c = 14.326(3)$ Å, $\beta = 90.56(3)°$, $U = 2243.1(8)$ Å^3, $Z = 4$, $D_c = 2.066$ Mg m^{-3}, $\lambda = 0.710\ 73$ Å, $T = 153(2)$ K, $\mu = 2.035$ mm^{-1}.

Data were collected on a Rigaku AFC7 diffractometer using an RS 3000 coated rapidly cooled crystal of dimensions 0.21 × 0.20 × 0.15 mm, mounted directly from solution, by the θ–ω method ($3 < 2\theta < 50°$). Of a total of 4169 reflections collected, 3948 were independent. The structure was solved by direct methods (SHELXL 93 and SHELXTL PLUS)[6] and refined by full-matrix least-squares analysis on F^2 with R_1 [$F > 4\sigma(F)$] and wR_2 (all data) 0.0295 and 0.0921, respectively.[7] The H atoms were placed in calculated positions and allowed to refine 'riding' on their C atoms. Largest peak and hole in final difference map 1.479 and −0.954 e Å^{-3}.

Crystal data for compound **3**. $C_{24}H_{18}O_9Ru_4$, $M = 854.66$, monoclinic, space group Cc, $a = 9.797(2)$, $b = 18.894(4)$, $c = 14.632(6)$ Å, $\beta = 104.79(2)°$, $U = 2\ 618.7(13)$ Å^3, $Z = 4$, $D_c = 2.168$ Mg m^{-3}, $\lambda = 0.710\ 73$ Å, $T = 293(2)$ K, $\mu = 2.315$ mm^{-1}.

Data were collected on a CAD 4 diffractometer using a crystal of dimensions 0.30 × 0.15 × 0.09 mm, mounted directly from solution, by the θ–ω method ($3 < 2\theta < 50°$). Of a total of 3262 reflections collected, 3261 were independent. Data were corrected for absorption using ψ scans ($T_{max} = 0.110$, $T_{min} = 0.058$). The structure was solved by direct methods (SHELXL 93 and SHELXTL PLUS)[6] and refined by full-matrix least-squares analysis on F^2 with R_1 [$F > 4\sigma(F)$] and wR_2 (all data) 0.0252 and 0.0661, respectively.[7] The H atoms were placed in calculated positions and allowed to refine 'riding' on their C atoms. Largest peak and hole in final difference map 0.581 and −1.335 e Å^{-3}.

Final atomic coordinates are given in Tables 4 and 5 respectively.

Table 5 Atomic coordinates (× 10^4) for compound **3**

Atom	x	y	z
Ru(2)	4 415(1)	8 987(1)	1 586(1)
Ru(4)	1 914(1)	8 972(1)	258(1)
Ru(1)	2 849(1)	7 666(1)	1 165(1)
Ru(3)	1 760(1)	8 810(1)	2 054(1)
C(1)	4 887(6)	7 175(3)	2 007(4)
C(2)	3 772(6)	6 699(3)	1 975(5)
C(3)	2 808(7)	7 020(3)	2 416(5)
C(4)	3 317(6)	7 699(3)	2 780(4)
C(5)	4 658(6)	7 802(3)	2 516(4)
C(6)	5 708(5)	8 351(3)	2 800(4)
C(7)	5 439(6)	9 019(3)	3 116(4)
C(8)	3 990(6)	9 227(3)	3 092(4)
C(9)	3 029(7)	8 845(4)	3 530(5)
C(10)	2 662(6)	8 138(3)	3 358(4)
C(11)	6 176(8)	7 041(4)	1 659(6)
C(12)	6 622(7)	9 532(4)	3 563(5)
C(13)	7 940(9)	9 462(6)	3 207(8)
C(14)	6 974(10)	9 434(5)	4 628(6)
C(15)	1 702(7)	7 794(4)	3 886(6)
C(202)	4 625(10)	9 950(4)	1 423(6)
O(202)	4 791(11)	10 533(3)	1 367(7)
C(201)	5 470(8)	8 834(4)	705(6)
O(201)	6 108(8)	8 771(4)	166(5)
C(401)	2 589(9)	9 031(4)	−863(6)
O(401)	3 020(10)	9 081(4)	−1 492(5)
C(402)	1 640(10)	9 932(4)	311(6)
O(402)	1 414(11)	10 523(3)	300(6)
C(403)	−17(9)	8 805(4)	−357(5)
O(403)	−1 192(7)	8 762(4)	−711(5)
C(101)	1 005(8)	7 415(4)	531(6)
O(101)	−72(7)	7 191(4)	161(6)
C(102)	3 286(8)	7 661(4)	−2(5)
O(102)	3 611(8)	7 528(4)	−688(5)
C(301)	910(7)	9 668(4)	2 109(5)
O(301)	359(7)	10 203(3)	2 145(6)
C(302)	−31(7)	8 423(4)	1 808(5)
O(302)	−1 127(6)	8 171(4)	1 689(6)

Additional material available from the Cambridge Crystallographic Data Centre comprises H-atom coordinates, thermal parameters and remaining bond lengths and angles.

Acknowledgements

We thank the University of Edinburgh and the EPSRC for financial support; NATO is acknowledged by D. B. and B. F. G. J. for a travel grant.

References

1 M. R. Churchill and P. H. Bird, *J. Am. Chem. Soc.*, 1968, **90**, 800; M. R. Churchill, K. Gold and P. H. Bird, *Inorg. Chem.*, 1969, **8**, 1956; M. R. Churchill, F. R. Scholer and J. Wormald, *J. Organomet. Chem.*, 1971, **28**, C21; M. R. Churchill and J. Wormald, *Inorg. Chem.*, 1973, **12**, 191.

2 D. Braga, F. Grepioni, E. Parisini, P. J. Dyson, B. F. G. Johnson, D. Reed, D. S. Shephard, P. J. Bailey and J. Lewis, *J. Organomet. Chem.*, 1993, **462**, 301; B. F. G. Johnson, C. Martin, D. Braga, F. Grepioni and E. Parisini, *J. Chem. Soc., Chem. Commun.*, 1994, 1253; B. F. G. Johnson, C. Martin, A. J. Blake and S. Ingham, unpublished work.

3 Ch. Elschenbroich, *Chem. Ber.*, 1984, **117**, 3165.

4 C. Krüger, *Angew. Chem., Int. Ed. Engl.*, 1969, **8**, 678.

5 D. Braga, P. J. Dyson, F. Grepioni, B. F. G. Johnson and M. J. Calhorda, *Inorg. Chem.*, 1994, **33**, 3218.

6 G. M. Sheldrick, SHELXL 93, Göttingen University, 1993; SHELXTL PLUS, version 4.2, Siemens Analytical Instruments Inc., Madison, WI, 1990.

7 T. Kottke and D. Stalke, *J. Appl. Crystallogr.*, 1993, **26**, 615.

Received 21*st March* 1995; *Paper* 5/01799H